Electronic Supplementary Information

Highly flexible tactile sensor with interlocked truncated sawtooth structure based on stretchable graphene/silver/silicone rubber composites

Yancheng Wang[*ab], *Lingfeng Zhu*[b], *Deqing Mei*[ab], *Wandong Zhu*[b]

[a]State Key Laboratory of Fluid Power and Mechatronic Systems, School of Mechanical Engineering, Zhejiang University, Hangzhou, 310027, China

[b]Key Laboratory of Advanced Manufacturing Technology of Zhejiang Province, School of Mechanical Engineering, Zhejiang University, Hangzhou, 310027, China

* Corresponding Author: yanchwang@zju.edu.cn

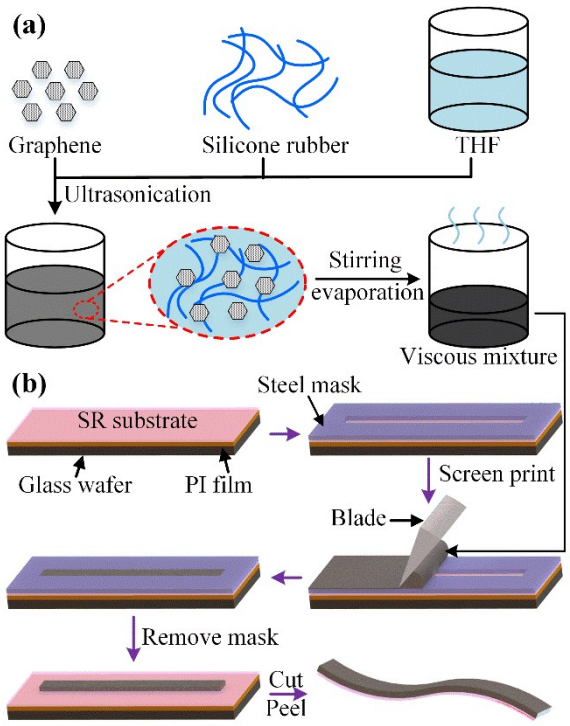

Fig. S1. (a) Preparation process of the GNP/SR composites, (b) fabrication method of the GNP/SR specimen.

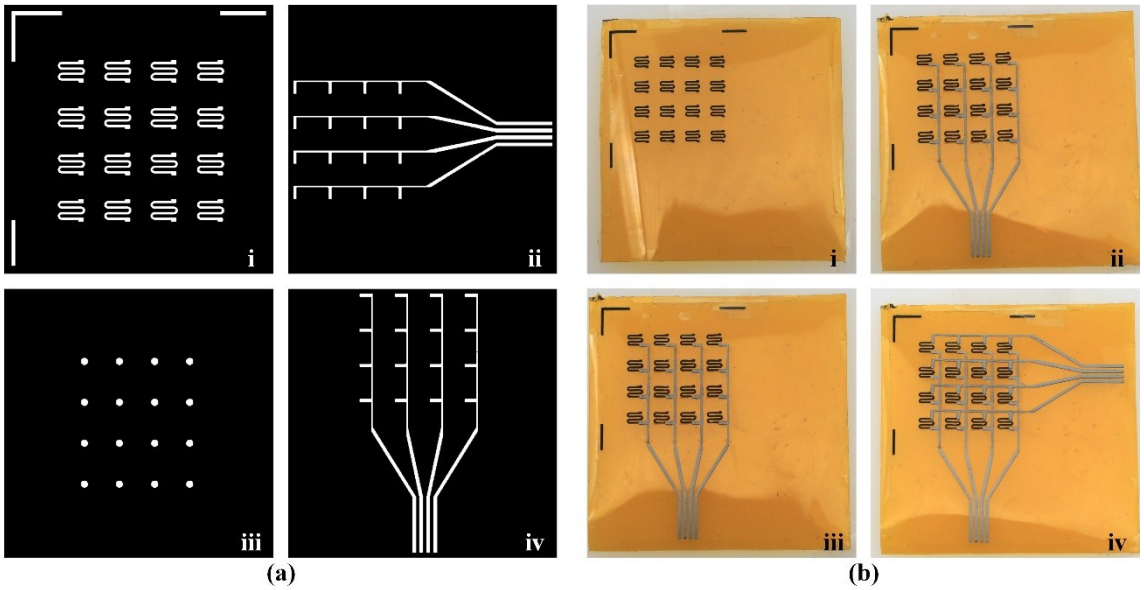

Fig. S2. The fabrication process of the graphene pattern and stretchable electrodes. (a) The mask for screen printing: i) graphene patterns, ii) row electrodes, iii) SR insulations, iv) column electrodes; (b) The corresponding fabricated layers: i) graphene patterns, ii) row electrodes, iii) SR insulations, iv) column electrodes.

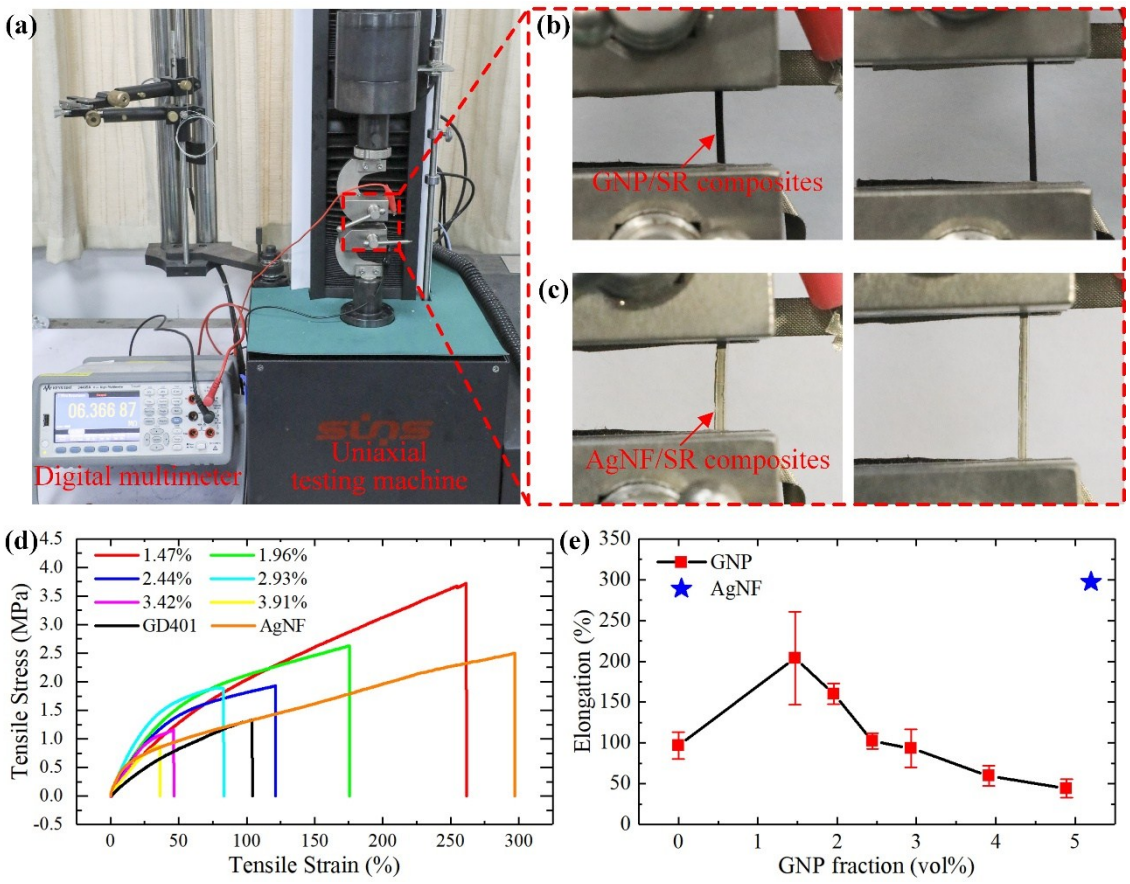

Fig. S3. Electromechanical property test of the GNP/SR and AgNF/SR composites. (a) The experimental setup contained a uniaxial testing machine and a digital multimeter. The specimen was connected to the multimeter by conductive tapes. (b) Images of the GNP/SR specimen during stretching. (c) Images of the AgNF/SR specimen during stretching. (d) The relationship between the tensile strain and stress of the specimens. (e) The elongations of the GNP/SR composites with different GNP volume fractions and the AgNF/SR composites.

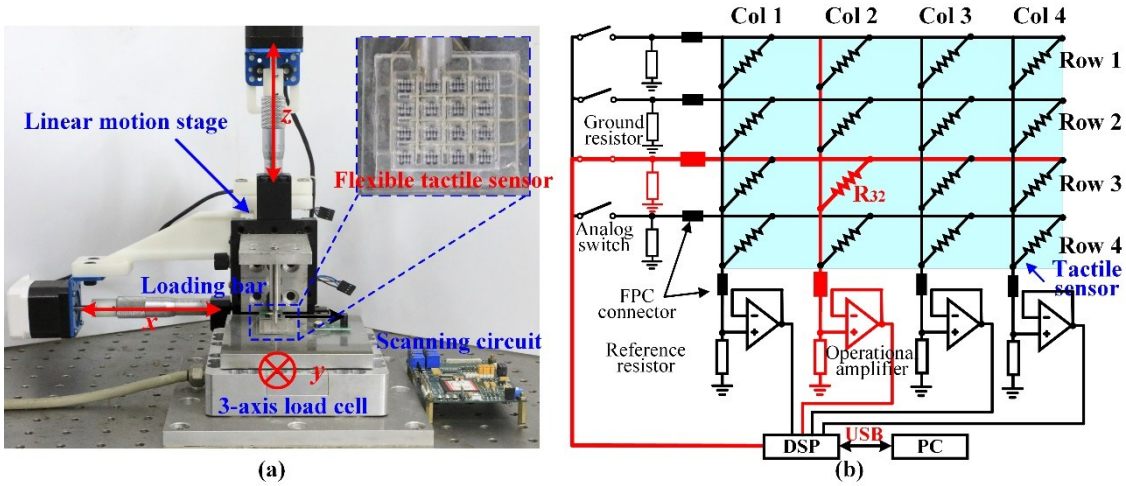

Fig. S4. (a) The home-made tactile sensing array calibration platform, including a three-dimensional linear motion stage and a 3-axis load cell with a resolution of 0.01 N. The tactile sensing array was connected to the scanning circuit through FPC connectors. (b) The schematic view of the scanning circuit. The analog switches were controlled by the DSP to select one row of the sensor for measurement. Three operational amplifiers were controlled to measure the resistance of the units in the sensor and transform it into voltage signals. Voltage signals were transmitted to a PC terminal for recording and further processing.

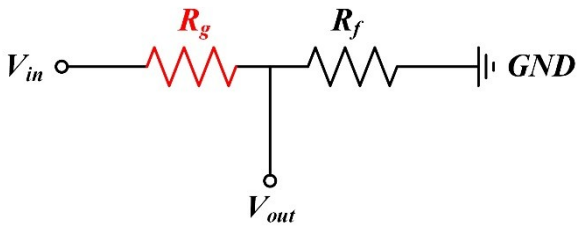

Fig. S5. The resistance measurement principle for one unit of the home-made circuit based on voltage divider.

This is a typical voltage divider circuit to transform the resistance change of the sensor into voltage signals and the output voltage can be calculated as:

$$V_{out} = \frac{R_f}{R_f + R_g} V_{in} \tag{1}$$

where V_{in} is the input voltage, V_{out} is the output voltage, R_f is the reference resistance, and R_g is the resistance of the sensor unit. According to the equation (1) and Fig. 5(b), the relationship between the resistance change and the applied pressure can be calculated. In our work, V_{in} = 3 V, R_f = 70 kΩ, and the size of a single unit is 4 mm × 4 mm. Therefore, the sensitivity of the sensor can be calculated as S_1 = 1.72% kPa^{-1} (3~94 kPa), and S_2 = 0.47% kPa^{-1} (94~125 kPa).

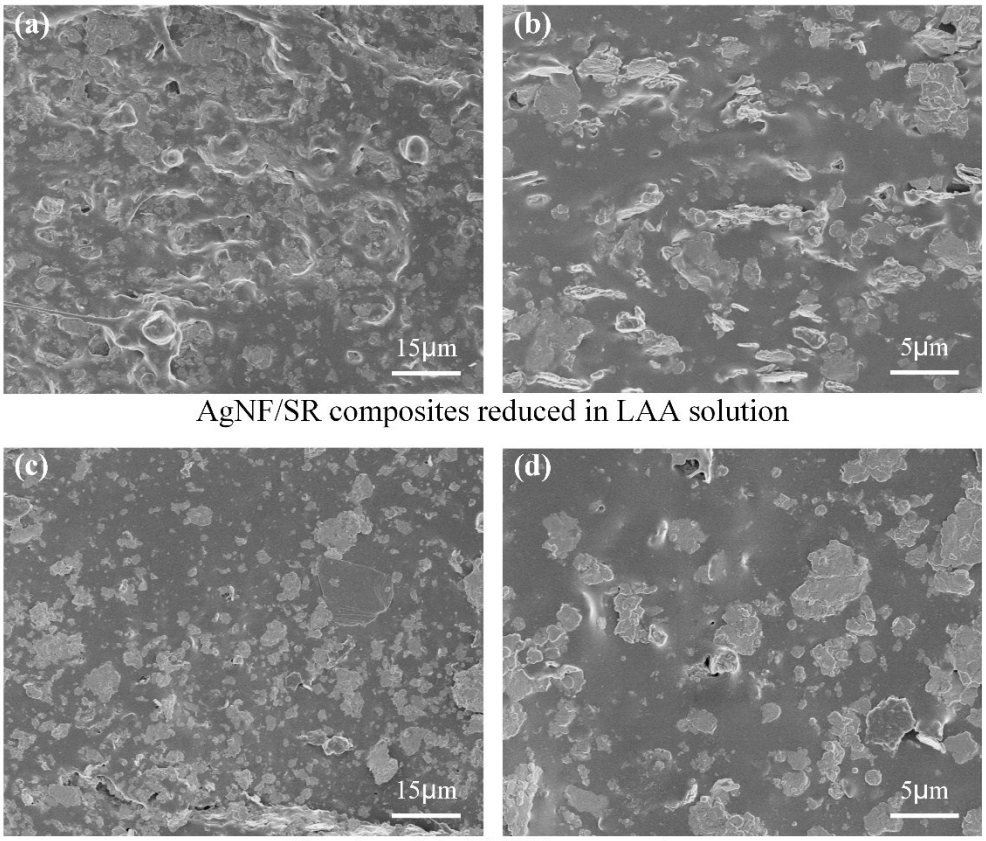

Fig. S6. The SEM images of the AgNF/SR composites after and before being reduced in LAA solution. (a-b) Reduced AgNF/SR composites under ×1000 and ×3000. (c-d) Unreduced AgNF/SR composites under ×1000 and ×3000.

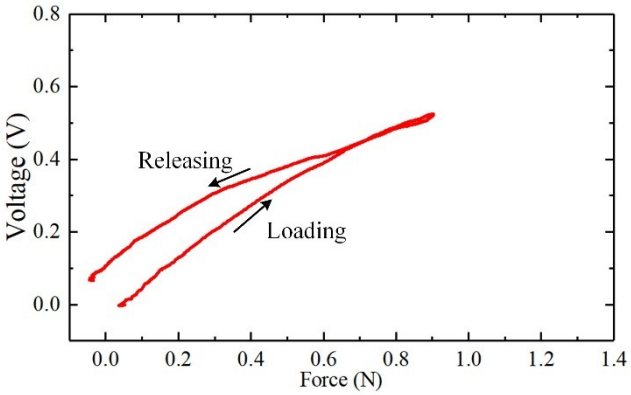

Fig. S7. The hysteresis effect of the tactile sensing unit. There is a 9% change in output voltage when the loading force of 0.9 N was released.

Table S1. Comparison on the gauge factor and stretchability of the piezoresistive composites between our work and the related research.

Materials	Gauge factor	Stretchability	Ref
Graphene foam-PDMS	29	70	(S1)
AuNWs-PANI	61.4	150	(S2)
GO-PEDOT-PU	193.2	550	(S3)
MWCNTs-PDMS	1140	10	(S4)
MWCNTs-Ecoflex	1378	330	(S5)
Graphene oxide woven fabrics-Natural rubber	3667	57	(S6)
CNT-Ecoflex	48	750	(S7)
rGO-VHB9410	150	82	(S8)
Pt-PU	30	150	(S9)
rGO-AgNPs	475	14.5	(S10)
AgNWs-PDMS	41.1	35	(S11)
Graphene woven fabrics	10^6	8	(S12)
Graphene foam-CNT-PDMS	20.5	85	(S13)
Carbonized silk georgette	173	100	(S14)
$Ti_3C_2T_x$-CNT	772.6	130	(S15)
AuNW-PU nanofiber-PDMS	2370	90	(S16)
AgNW-Elastomer	81	150	(S17)
AgNP-AgNW-PDMS	3766	28.1	(S18)
AgNW/PU	9557	150	(S19)
SWCNT-Thermoplastic elastomer	425	100	(S20)
AuNW-AgNW-PDMS	236	70	(S21)
Pt nanobelt	4000	160	(S22)
Carbon nanocoil-PDMS	190	260	(S23)
Pt-PDMS	2000	2	(S24)
Our work	**13692**	**170**	

Table S2. Comparison on the pressure sensitivity and sensing range of the piezoresistive sensors between our work and the related research.

Type	Materials	Sensitivity	Sensing range	Ref
Piezoresistive	Graphene-PAS	1.1% kPa^{-1}	30 kPa	(S25)
Piezoresistive	Silicon nanoribbon-PDMS	0.41% kPa^{-1}	200 kPa	(S26)
Piezoresistive	AgNW-Elastomer	0.3% kPa^{-1}	200 kPa	(S17)
Piezoresistive	Carbon nanocoil-PDMS	0.076% kPa^{-1}	100 kPa	(S23)
Piezoresistive	Graphene-PI	18% kPa^{-1}	7 kPa	(S27)
Piezoresistive	RGO-Silk fabric	0.4% kPa^{-1}	180 kPa	(S28)
Capacitive	Cu/Ni nanofiber-PDMS	1.7% kPa^{-1}	250 kPa	(S29)
Capacitive	AgNW-PDMS	0.39% kPa^{-1}	1.3 MPa	(S30)
Capacitive	Graphene-PVC	1% kPa^{-1}	80 kPa	(S31)
Capacitive	AgNF-AgNW	0.18% kPa^{-1}	1.6 MPa	(S32)
Piezoelectric	$PbTiO_3$NW-Graphene	0.94% kPa^{-1}	1.4 kPa	(S33)
Triboelectric	ITO-Graphene FET-PDMS	2% kPa^{-1}	57 kPa	(S34)
Piezoresistive	**Graphene-AgNF-SR**	**1.72% kPa^{-1} (3~94 kPa)** **0.47% kPa^{-1} (94~125 kPa)**	**3 ~ 125 kPa**	**Our work**

References

1. Y. R. Jeong, H. Park, S. W. Jin, S. Y. Hong, S.-S. Lee and J. S. Ha, *Adv. Funct. Mater.*, 2015, **25**, 4228-4236.
2. S. Gong, D. T. H. Lai, Y. Wang, L. W. Yap, K. J. Si, Q. Shi, N. N. Jason, T. Sridhar, H. Uddin and W. Cheng, *ACS Appl. Mater. Interfaces*, 2015, **7**, 19700-19708.
3. K. Qi, J. He, H. Wang, Y. Zhou, X. You, N. Nan, W. Shao, L. Wang, B. Ding and S. Cui, *ACS Appl. Mater. Interfaces*, 2017, **9**, 42951-42960.
4. B. Nie, X. Li, J. Shao, X. Li, H. Tian, D. Wang, Q. Zhang and B. Lu, *ACS Appl. Mater. Interfaces*, 2017, **9**, 40681-40689.
5. Z. Tang, S. Jia, F. Wang, C. Bian, Y. Chen, Y. Wang and B. Li, *ACS Appl. Mater. Interfaces*, 2018, **10**, 6624-6635.
6. B. Yin, Y. Wen, T. Hong, Z. Xie, G. Yuan, Q. Ji and H. Jia, *ACS Appl. Mater. Interfaces*, 2017, **9**, 32054-32064.
7. S.-J. Park, J. Kim, M. Chu and M. Khine, *Adv. Mater. Technol.*, 2016, **1**, 1600053.
8. Q. Liu, J. Chen, Y. Li and G. Shi, *ACS Nano*, 2016, **10**, 7901-7906.
9. H. Jeon, S. K. Hong, M. S. Kim, S. J. Cho and G. Lim, *ACS Appl. Mater. Interfaces*, 2017, **9**, 41712-41721.
10. Z. Yang, D.-Y. Wang, Y. Pang, Y.-X. Li, Q. Wang, T.-Y. Zhang, J.-B. Wang, X. Liu, Y.-Y. Yang, J.-M. Jian, M.-Q. Jian, Y.-Y. Zhang, Y. Yang and T.-L. Ren, *ACS Appl. Mater. Interfaces*, 2018, **10**, 3948-3954.
11. J. H. Cho, S.-H. Ha and J.-M. Kim, *Nanotechnology*, 2018, **29**, 155501.
12. T. Yang, X. Jiang, Y. Zhong, X. Zhao, S. Lin, J. Li, X. Li, J. Xu, Z. Li and H. Zhu, *Acs Sens.*, 2017, **2**, 967-974.
13. Y. Cai, J. Shen, Z. Dai, X. Zang, Q. Dong, G. Guan, L.-J. Li, W. Huang and X. Dong, *Adv. Mater.*, 2017, **29**, 1606411.
14. C. Wang, K. Xia, M. Jian, H. Wang, M. Zhang and Y. Zhang, *J. Mater. Chem. C*, 2017, **5**, 7604-7611.
15. Y. Cai, J. Shen, G. Ge, Y. Zhang, W. Jin, W. Huang, J. Shao, J. Yang and X. Dong, *ACS Nano*, 2018, **12**, 56-62.
16. S. Duan, Z. Wang, L. Zhang, J. Liu and C. Li, *Adv. Mater. Technol.*, 2018, **3**, 1800020.
17. K.-H. Kim, N.-S. Jang, S.-H. Ha, J. H. Cho and J.-M. Kim, *Small*, 2018, **14**, 1704232.
18. S. Sang, L. Liu, A. Jian, Q. Duan, J. Ji, Q. Zhang and W. Zhang, *Nanotechnology*, 2018, **29**, 255202.
19. Z. Cao, R. Wang, T. He, F. Xu and J. Sun, *ACS Appl. Mater. Interfaces*, 2018, **10**, 14087-14096.
20. J. Zhou, X. Xu, Y. Xin and G. Lubineau, *Adv. Funct. Mater.*, 2018, **28**, 1705591.
21. M. D. Ho, Y. Ling, L. W. Yap, Y. Wang, D. Dong, Y. Zhao and W. Cheng, *Adv. Funct. Mater.*, 2017, **27**, 1700845.
22. Y. Wang, J. Cheng, Y. Xing, M. Shahid, H. Nishijima and W. Pan, *Small*, 2017, **13**, 1604291.
23. C. Deng, L. Pan, D. Zhang, C. Li and H. Nasir, *Nanoscale*, 2017, **9**, 16404-16411.
24. D. Kang, P. V. Pikhitsa, Y. W. Choi, C. Lee, S. S. Shin, L. Piao, B. Park, K.-Y. Suh, T.-i. Kim and M. Choi, *Nature*, 2014, **516**, 222-226.
25. S. Chun, Y. Choi, D. I. Suh, G. Y. Bae, S. Hyun and W. Park, *Nanoscale*, 2017, **9**, 10248-10255.
26. J. Kim, M. Lee, H. J. Shim, R. Ghaffari, H. R. Cho, D. Son, Y. H. Jung, M. Soh, C. Choi, S. Jung, K. Chu, D. Jeon, S.-T. Lee, J. H. Kim, S. H. Choi, T. Hyeon and D.-H. Kim, *Nat. Commun.*, 2014, **5**, 5747.
27. Y. Qin, Q. Peng, Y. Ding, Z. Lin, C. Wang, Y. Li, J. Li, Y. Yuan, X. He and Y. Li, *ACS Nano*, 2015,

9, 8933-8941.
28. J. F. Saenz-Cogollo, M. Pau, B. Fraboni and A. Bonfiglio, *Sensors*, 2016, **16**, 365.
29. J. Wang, R. Suzuki, M. Shao, F. Gillot and S. Shiratori, *ACS Appl. Mater. Interfaces*, 2019, **11**, 11928-11935.
30. N. Chou, Y. Kim and S. Kim, *ACS Appl. Mater. Interfaces*, 2016, **8**, 6269-6276.
31. C. G. Nunez, W. T. Navaraj, E. O. Polat and R. Dahiya, *Adv. Funct. Mater.*, 2017, **27**, 1606287.
32. B. W. An, S. Heo, S. Ji, F. Bien and J.-U. Park, *Nat. Commun.*, 2018, **9**, 2458.
33. Z. Chen, Z. Wang, X. Li, Y. Lin, N. Luo, M. Long, N. Zhao and J.-B. Xu, *ACS Nano*, 2017, **11**, 4507-4513.
34. U. Khan, T.-H. Kim, H. Ryu, W. Seung and S.-W. Kim, *Adv. Mater.*, 2017, **29**, 1603544.